Appendix B

Introduction to biomedical electrical impedance tomography

David Holder

One of the attractions but also difficulties of biomedical EIT is that it is interdisciplinary. Topics which are second nature to one discipline may be incomprehensible to those with other backgrounds. Not all readers will be able to follow all the chapters in this book, but I hope that the majority will be comprehensible to most, especially those with a medical physics or bioengineering background. Nevertheless, the reconstruction algorithm or instrumentation chapters may be difficult to follow for clinical readers, and some of the clinical terminology and concepts in application chapters may be unfamiliar to readers with Maths or Physics backgrounds. This chapter is intended as a brief and non-technical introduction to biomedical electrical impedance tomography. It is didactic and explanatory, so that the more detailed chapters in the book which follow may be easier to follow for the general reader. It is intended to be comprehensible to readers with clinical or life sciences backgrounds, but with the equivalent of high school physics. A non-technical introduction to the basics of bioimpedance is presented as an appendix, and may be helpful for any reader wishing to refresh their understanding of the basics of electricity and its flow through biological tissues. As it is intended to be explanatory, key references and suggestions for further reading are included, but the reader is recommended to the detailed chapters in the main body of the book for detailed citations.

B.1. HISTORICAL PERSPECTIVE

The first published impedance images appear to have been those of Henderson and Webster in 1976 and 1978 (Henderson and Webster 1978). Using a rectangular array of 100 electrodes on one side of the chest earthed with a single large electrode on the other side, they were able to produce a transmission image of

the tissues. Low conductivity areas in the image were claimed to correspond to the lungs. Shortly after, an impedance tomography system for imaging brain tumours was proposed by Benabid *et al* (1978). They reported a prototype impedance scanner which had two parallel arrays of electrodes immersed in a saline filled tank, and which was able to detect an impedance change inserted between the electrode arrays.

The first clinical impedance tomography system, then called applied potential tomography (APT), was developed by Brian Brown and David Barber and colleagues in the Department of Medical Physics in Sheffield. They produced a celebrated commercially available prototype, the Sheffield mark 1 system (Brown and Seagar 1987), which has been widely used for performing clinical studies, and is still in use in many centres today. This system made multiple impedance measurements of an object by a ring of 16 electrodes placed around the surface of the object.

The first published tomographic images were from this group in 1982 and 1983. They showed images of the arm in which areas of increased resistance roughly corresponded to the bones and fat. As EIT was developed, images of gastric emptying, the cardiac cycle and the lung ventilation cycle in the thorax were obtained and published. The Sheffield EIT system had the advantage that 10 images/s could be obtained, the system was portable, and the system was relatively inexpensive compared to ultrasound, CT and MRI scanners. However, since the EIT images obtained were of low resolution compared to other clinical techniques such as cardiac ultrasound and x-ray contrast studies of the gut, EIT did not gain widespread clinical acceptance (see Holder 1993, Boone *et al* 1997, Brown, 2003, for reviews).

Around the same time, a group in Oxford proposed that EIT could be used to image the neonatal brain (Murphy *et al* 1987). They developed a clinical EIT system and obtained preliminary EIT images in two neonates. Their system used 16 electrodes placed in a ring around the head, but in contrast to the Sheffield system, the current was applied to the head by pairs of electrodes which opposed each other in the ring in a polar drive configuration. This maximized the amount of current which entered the brain and therefore maximized the sensitivity of the EIT system to impedance changes in the brain.

Since the first flush of interest in the mid to late 1980s, about a dozen groups have developed their own EIT systems and reconstruction software, and publications on development and clinical applications have been produced by perhaps another 20 or so. Initial interest in a wide range of applications at first has now settled into the main areas of imaging lung ventilation, cardiac function, gastric emptying, brain function and pathology, and screening for breast cancer. Convincing pilot and proof of principle studies have been performed in these areas. In 1999, FDA approval was given to a method of impedance scanning to detect breast cancer, and the system has been marketed commercially (http://imaginis.com/t-scan/effectiveness.asp),

but it is not yet clear how widely it is being used. In other areas, EIT has not yet broken into routine clinical use.

B.2. EIT INSTRUMENTATION

EIT systems are generally about the size of a video recorder, but some may be larger. They usually comprise a box of electronics and a PC. Connection to the subject is usually made by coaxial cables a metre or two long, and ECG type electrodes are placed in a ring or rings on the body part of interest. All will sit on a movable trolley, so that recording can be made in a clinic or out-patient department. A typical system is shown in figure B.1.

B.2.1. Individual impedance measurements

A single impedance measurement forms the basis of the data set which is used to reconstruct an image. Most systems use a four-electrode method, in which constant current is applied to two electrodes, and the resulting voltage is recorded at two others. This minimizes the errors due to electrode impedance. The transfer impedance of the subject with this recording geometry is calculated using Ohm's law (figure B.2). The current applied is approximately one tenth of the threshold for causing sensation on the skin. It is insensible and has no known ill effects. Most single frequency systems apply a current at about 50 kHz. At this frequency, the properties of tissue are similar to those at d.c., in that the great majority of current travels in the extracellular space, but electrode impedance is much lower than at d.c., so there are less instrumentation errors. At 50 kHz, a single measurement usually takes less than 1 msec.

Figure B.1. The Sheffield mark 2 EIT system (Sinton *et al* 1992).

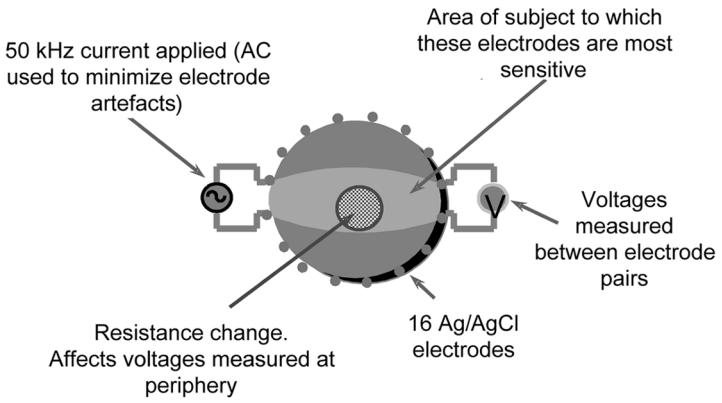

Figure B.2. Typical single impedance measurement with EIT.

The electronics for this four-electrode arrangement comprises a current source, a voltage recording circuit, and a means to extract the phase sensitive information from the acquired voltage. The latter usually employs a circuit called a phase-sensitive demodulator. The phase of the injected current is known; the circuit retrieves the value of the received waveform both in-phase with the applied current and with a phase delay of 90°. In this way, the resistance and reactance may be calculated (figure B.3). Many systems discard the out-of-phase component, as it may be inaccurate due to effects of stray capacitance. Early systems, such as the Sheffield mark 1, used a single such impedance measuring circuit, which was then linked to the electrodes by a multiplexer. More recent systems use multiple circuits for drive and receive, which increases the speed of acquisition but also expense and bulk.

It will be seen below that EIT images in human subjects suffer from low resolution. One of the causes is errors in individual measurements. The principal of these is a high skin-electrode impedance. In principle, measurement should be accurate with a four-electrode system. Unfortunately, in practice, this is not the case. It is generally necessary to abrade the skin of subjects to lower the impedance, and this can easily vary from site to site. Although leads are coaxial, and usually have driven screens to minimize stray capacitance, this is significant, especially at higher frequencies. The combination of variable skin impedance and stray capacitance conjoin to cause significant errors in recorded impedance values, especially in electrode combinations which are recording small voltages. Significant factors include fluctuations in current delivered, if skin impedances vary at different electrodes, and

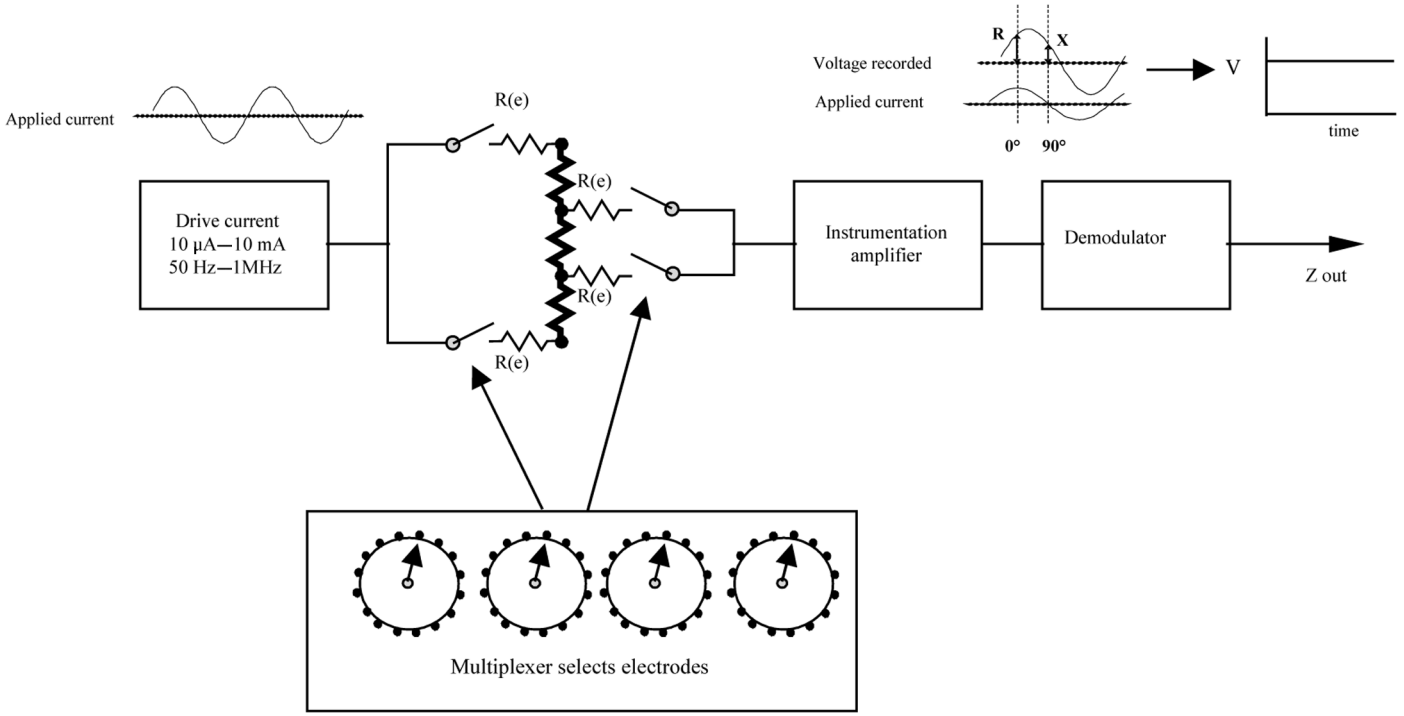

Figure B.3. Essential components of an EIT system. The system shown is for a single impedance measuring circuit with connection to electrodes using a multiplexer. More complex systems may have multiple circuits attached directly to electrode pairs. The demodulator converts the a.c. recorded signal into a steady d.c. voltage for both resistance and reactance, although the reactance signal is discarded in many systems as the stray capacitance renders it inaccurate. The subject and electrode impedances (R(e)) are represented as resistances.

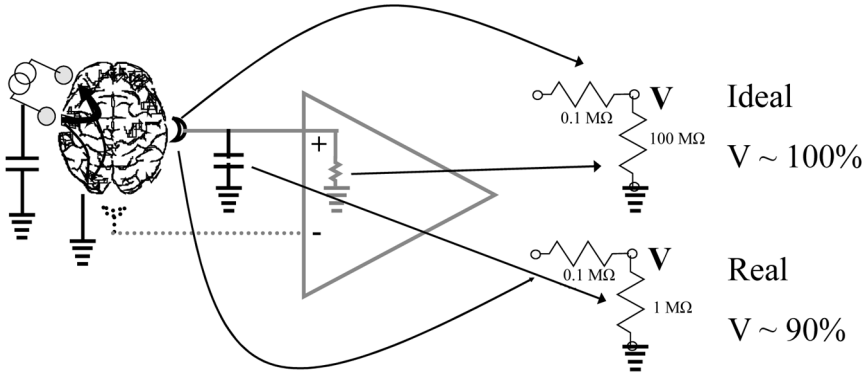

Figure B.4. Sources of error in impedance measurements. There are two main sources of error. (1) A voltage divider exists, formed by the series impedance of the skin and input impedance of the recording instrumentation amplifier. Under ideal circumstances, the skin impedance is negligible compared to the input impedance of the amplifier, so that the voltage is very accurately recorded (upper example). In this example, skin importance is 100 kOhms and input impedance is 100 MOhms, so the loss of signal is negligible. In practice, the stray capacitance in the leads, coupled to high skin impedances, may cause a significant attenuation of the voltage recorded—e.g. to 90%, if the input impedance reduces to 1 MOhm (lower example). In this diagram, only one side of a differential amplifier is shown, for clarity. This attenuating effect may be different for the two sides of the amplifier. This leads to a loss of common mode rejection ability, as well as absolute errors in the amplitude recorded. (2) The ideal current source is perfectly balanced, so that all current injected leaves by the sink of the circuit. The effect of stray capacitance and skin impedance may act to unbalance the current source. Some current then finds its way to ground, either by the ground, or by the high input impedance of the recording circuit. This causes a large common mode error. The common mode rejection ratio may be poor because of the effects in (1), so that the recorded voltage is inaccurate.

common mode errors on the recording side due to impaired common mode rejection as a result of stray capacitance (see Boone and Holder 1996 for a review) (figure B.4).

B.2.2. Data collection

EIT systems employ from eight to 64 electrodes. Earlier systems used 16 electrodes applied in a ring, but current systems may use several rings on the thorax or evenly distributed, for example, over the head. The following describes the procedure employed by a standard early prototype, the Sheffield mark 1 system (Brown and Seagar 1987). Sixteen electrodes are applied in a ring. A single measurement is made with four electrodes. A current of up to 5 mA at 50 kHz is applied between an adjacent pair of electrodes, and the voltage difference is recorded from two other adjacent electrodes. This yields a single transfer impedance measurement. Only the

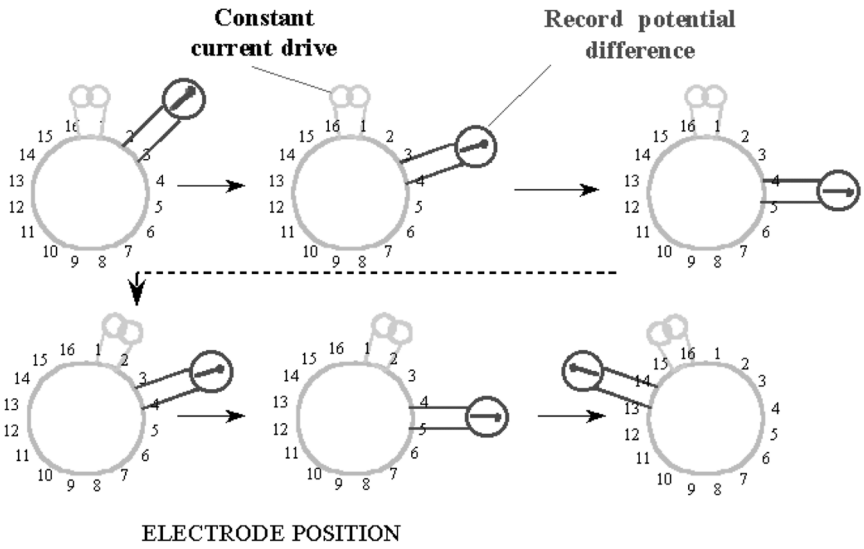

Figure B.5. Data acquisition with the Sheffield mark 1 system. A constant current is injected into the region between two adjacent electrodes, and the potential differences between all other pairs of adjacent electrodes are measured. The current drive is then moved to the next pair of adjacent electrodes, and the measurements repeated and so on for all possible current drive pairs. It is not possible to measure potential differences accurately at the pair of electrodes injecting current, so there are 208 (13×16) measurements in a data set.

in-phase component of the voltage is recorded, so this is a recording of resistance, rather than impedance. Voltage signals are measured on all other electrodes in turn (figure B.5). Sequential pairs are then successively used for injecting current until all possible combinations have been measured. Each individual measurement takes less than a millisecond, so a complete data set of 208 combinations is collected in 80 ms, and 10 images/s can be acquired. This can be increased to 25 frames/s if reciprocal electrode combinations are not used, and each data set comprises 104 measurements.

About 20 different designs have been constructed and reported since the Sheffield mark 1 system in 1984. Many were very similar, but had variations such as a variable software selectable variable frequency, miniaturization (figure B.6) (Baisch 1993), or a design with a separate headbox on a long lead to enable recording over days in ambulatory patients (figure B.7) (Yerworth *et al* 2002).

In theory, greater resolution within the image can be obtained if current is injected from many electrodes at once. This may be injected in different combinations to give fixed patterns of increasing spatial frequency, as in designs from groups at the Rensellaer Polytechnic (RPI), New York, USA

Figure B.6. Miniature Sheffield mark 1 APT system designed for the Juno space mission (courtesy of Prof. B. Brown).

(Cook *et al* 1994), Oxford Brookes University, Oxford, UK (Zhu *et al* 1993), or Dartmouth, USA (Halter *et al* 2004). It has also been proposed that the patterns may be automatically adjusted to give the best image accuracy (Zhu *et al* 1994). Although these approaches are better in theory, this requires

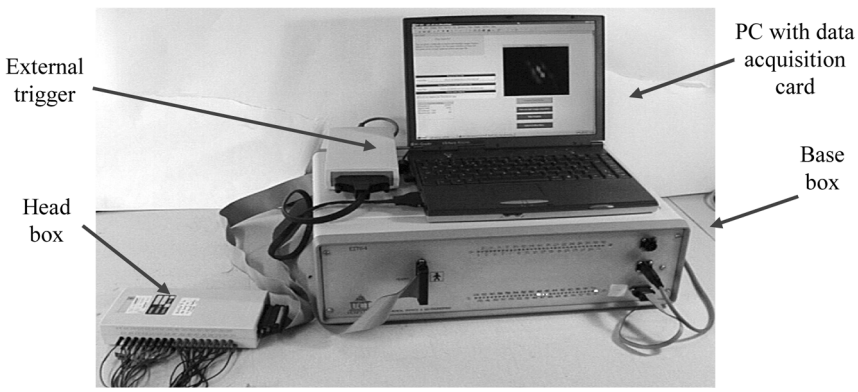

Figure B.7. UCLH mark 1 EIT system, intended for ambulatory recording in subjects being monitored on a ward for epileptic seizures. A small headbox is on a lead 10 m long, so that the subject may walk around near their bed during recording.

much greater precision as all the current sources have to be controlled accurately at once; it is not yet clear if, in practice, this confers an improvement in image quality over the simpler method of applying current only to two electrodes at a time. Other variations in hardware design include applying voltage and measuring current, using only two rather than four electrodes for individual measurements as in the RPI system, or recording many frequencies simultaneously—multifrequency EIT or EIT spectroscopy (EITS).

B.2.3. Electrodes

The great majority of clinical measurements have been made with ECG type adhesive electrodes attached to the chest or abdomen (figure B.1). Although the four-electrode recording system should in theory be immune to electrode-skin impedance, in practice it is usually necessary to first reduce the skin impedance by abrasion. Similar EEG cup electrodes have been used for head recording.

In the mid 1980s convenient flexible electrode arrays were designed and reported for chest imaging, but did not become commercially available, so now most groups use ECG or EEG electrodes (McAdams *et al* 1994). Some specialized designs have been developed for the special case of imaging the breast—precise positioning may be achieved by radially movable motorized rods arranged in a circle (figure B.8).

B.2.4. Setting up and calibrating measurements

Data collection in human subjects in EIT is sensitive to movement artefact and the skin-electrode impedance. It is usually necessary, therefore, to check signal quality before embarking on recordings. A simple widely used method is to check electrode impedance. Another method, pioneered by the Sheffield mark 1 system, is to measure 'reciprocity'. This principle is that the recorded transfer impedance should be the same, under ideal circumstances, if the recording and drive pair are reversed. A low reciprocity ratio—usually below 80%—generally indicates poor skin contact, which can be corrected by further skin abrasion or repositioning of the electrodes. Other systems, especially those using two, rather than four, electrodes may require special trimming before recording. Another potential problem lies in determining the correct zero phase setting for the impedance measuring circuit. The phase of the current produced by the electronics is, of course, accurately known, but stray capacitance and skin impedance may interact to alter the zero phase of the current delivered to the subject, and similar effects on the recording side may also alter the phase of the signal delivered to the demodulator. Different approaches have been employed. One method is to calibrate the system on a saline filled tank. Others are to optimize the

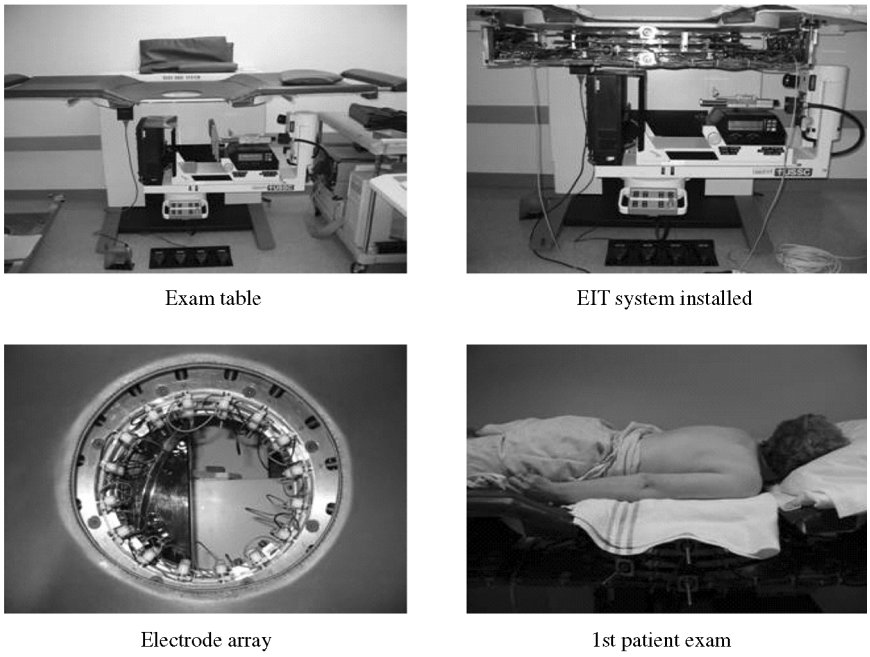

Figure B.8. A system for EIT of the breast. (Courtesy of Prof. A. Hartov, Dartmouth, USA.)

reciprocity, or to assume that the subject is primarily resistive at low frequencies, and adjust the phase detection accordingly (Fitzgerald *et al* 2002).

As many EIT systems are prototypes, it is helpful to calibrate them on known test objects. Some employ agar test objects, impregnated with a saline solution, in a larger tank which contains saline of a different concentration. These can be accurate if images are made quickly, but the saline will diffuse into the bathing solution, so that the boundaries can become uncertain (Cook *et al* 1994). Others have employed a porous test object such as a sponge, immersed in the bathing solution in a tank, so that the impedance contrast is produced by the presence of the insulator in the test object (Holder *et al* 1996a). Many tanks have been cylindrical; more realistic ones have simulated anatomy, such as the head (Tidswell *et al* 2003), or used biological materials to produce multifrequency test objects. Typically, the spatial resolution of test objects in tanks is about 15% of the image diameter (figure B.9).

B.2.5. Data collection strategies

Most EIT work has used EIT as a dynamic imaging method, in which images of the impedance change compared to a baseline condition are obtained. An

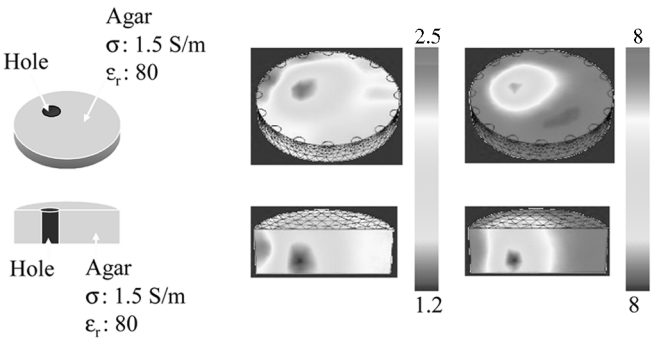

Figure B.9. Example of image quality with a modern multifrequency EIT system from Dartmouth, USA. (Courtesy of Prof. A. Hartov.)

example is EIT of gastric emptying. A reference baseline image is obtained at the start of the study when the stomach is empty. The stomach is then filled when the subject drinks a conductive saline solution (figure B.10). Subsequent EIT images are reconstructed with reference to the baseline image, and demonstrate the impedance change as the stomach fills and then empties the conductive solution. A second example is of cardiac imaging: images are gated to the electrocardiogram (ECG) to demonstrate the change in impedance during systole, when the heart is full of blood in the cardiac cycle, compared to a reference baseline image when the heart is emptied of blood in diastole (figure B.11). To image ventilation, a reference image is obtained when the lungs are partially emptied of air at the end of expiration and EIT images of the changes during normal ventilation are reconstructed with reference to the baseline image.

The main reason for imaging dynamic impedance changes is to eliminate or reduce errors that occur due to the instrumentation or differences

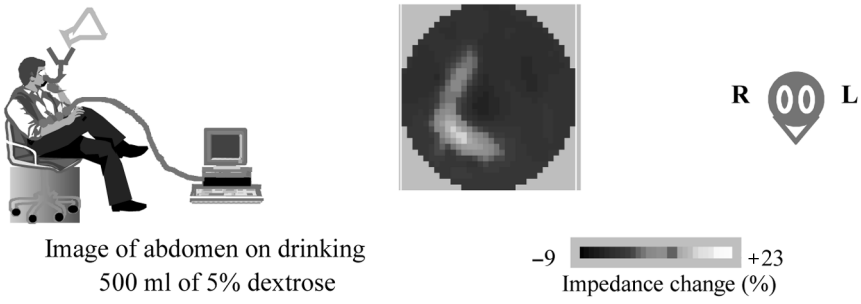

Figure B.10. Example of EIT of gastric emptying, collected with the Sheffield mark 1 EIT system, and 16 electrodes placed around the abdomen.

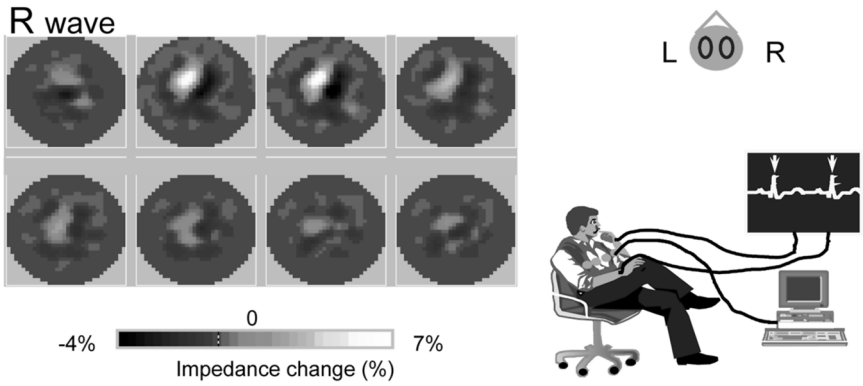

Figure B.11. Example of cardiac imaging, collected with the Sheffield mark 1 EIT system, and a ring of 16 electrodes placed around the chest.

between the model of the body part used in the reconstruction software and the actual object imaged. To reduce these, impedance changes are reconstructed with reference to a baseline condition; if the electrode placement errors in the baseline images and the impedance change images are the same, then these errors largely cancel if only impedance change is imaged. Although the dynamic imaging approach minimizes reconstruction errors, it limits the application of EIT to experiments in which an impedance change occurs over a short experimental time course; otherwise, electrode impedance drift may introduce artefacts in the data which cannot be predicted from the baseline condition. As dynamic imaging cannot be used to image objects present at the start of imaging and therefore in the baseline images, dynamic EIT cannot be used to obtain images of tumours or cysts. This contrasts with images obtained with CT, which can obtain static images of contrasting tissues such as tumours. Dynamic imaging has been used for almost all clinical studies to date in all areas of the body.

In principle, it should be possible to produce images of the absolute impedance. Unfortunately, image production is sensitive to errors in instrumentation and between the model used in reconstruction and the object imaged. Pilot data has been obtained in tanks (Cook *et al* 1994) and some preliminary images in human subjects (Cherepenin *et al* 2002, Soni *et al* 2004).

Dynamic EIT images typically use one measurement frequency, usually between 10 and 50 kHz, to make impedance measurements. An alternative approach is to compare the difference between impedance images measured at different measurement frequencies, termed EITS (EIT spectroscopy). This technique exploits the different impedance characteristics of tissues

at different measurement frequencies. An example of such a contrast would be the difference between cerebro-spinal fluid (CSF) and the grey matter of the brain. As the CSF is an acellular, ionic solution, it can be considered a pure resistance, so that its impedance is identical and equal to the resistance for all frequencies of applied current. However, the grey matter, which has a cellular structure, has a higher impedance at low frequencies than at high frequencies This frequency difference can theoretically be exploited to provide a contrast in the impedance images obtained at different frequencies, and provides a means of identifying different tissues in a multifrequency EIT image. The Sheffield mark 3.5 is an example (Hampshire *et al* 1995, Yerworth *et al* 2003). Eight electrodes are used in an adjacent drive/receive protocol to deliver sine waves at frequencies between 2 kHz and 1.6 MHz; Cole parameters such as the centre frequency and ratio of intra- to extra-cellular space can be extracted to create images.

B.3. EIT IMAGE RECONSTRUCTION

B.3.1. Back-projection

The hardware described above produces a series of measurements of the transfer impedance of the subject. These may be transformed into a tomographic image using similar methods to x-ray CT. The earliest method, employed in the Sheffield mark 1 system, is most clear intuitively. Each measurement may be conceived as similar to an x-ray beam—it indicates the impedance of a volume between the recording and drive electrodes. Unfortunately, unlike x-rays, this is not a neat defined beam, but a diffuse volume which has graded edges. Nevertheless, a volume of maximum sensitivity may be defined. The change in impedance recorded with each electrode combination is then back-projected into a computer simulation of the subject—a 2D circle for the Sheffield mark 1. The back-projected sets will overlap to produce a blurred reconstructed image, which can then be sharpened by the use of filters (figure B.12).

B.3.2. Sensitivity matrix approaches

Back-projection has been very successful for the simple case of 16 electrodes in a plane, but suffered from the need for two assumptions—that the problem was 2D, and that the initial resistivity was uniform. Most systems now employ a more powerful method, based on a ‘sensitivity matrix’ (figure B.13). This is based on a matrix, or table, which relates the resistivity of each voxel in the subject, and hence, images, to the recorded voltage measurements.

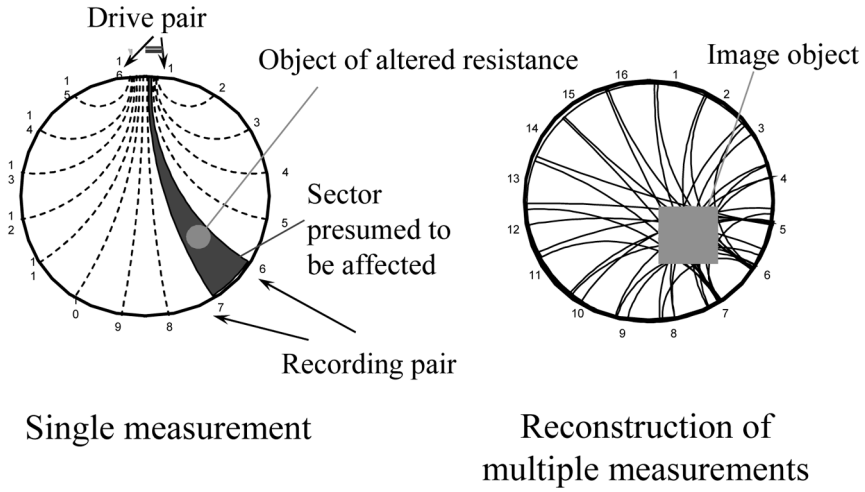

Figure B.12. Principles of EIT image reconstruction by back-projection.

The method requires a mathematical model of the body part of interest. These may be modelled using mathematical formulae alone—these are termed 'analytical' solutions. In general, these are only practical for simple shapes, such as a cylinder or sphere. More realistic shapes, such as the thorax or head containing layers representing the internal anatomy, are achieved using imaginary meshes in the model, whose boundaries are determined by segmenting MRI or CT images. The equations of current flow are solved for each cell in the mesh; each cell's calculation is therefore simple, but solutions for the whole mesh, which may contain tens of thousands of cells, may be time consuming on even powerful computers, and may suffer from instability or hidden quantitative errors. These are termed 'numerical' methods and common mesh types are FEM (finite element mesh) or BEM (boundary element mesh).

Using one of these models, the expected voltages at each electrode combination can be calculated. The principle is that the applied current actually flows everywhere in the subject, but, clearly, flows more in certain regions than others. Each voxel in the subject contributes to the voltage measured at a specified recording pair, but this depends on the resistance in the voxel, the amount of current which reaches it, and its distance from the recording electrodes. The total voltage at the recording pair is a sum of all these contributions from every voxel. Many of these, from voxels far away, may be negligible. This is illustrated in figure B.13(a), for the case of a disc with just four voxels. In practice, for 16 or 32 electrode systems, several hundred electrode combinations are recorded, so the matrix will have several hundred rows. In principle, an image can only be accurately reconstructed if there is one independent measurement for each voxel. In practice, accurate

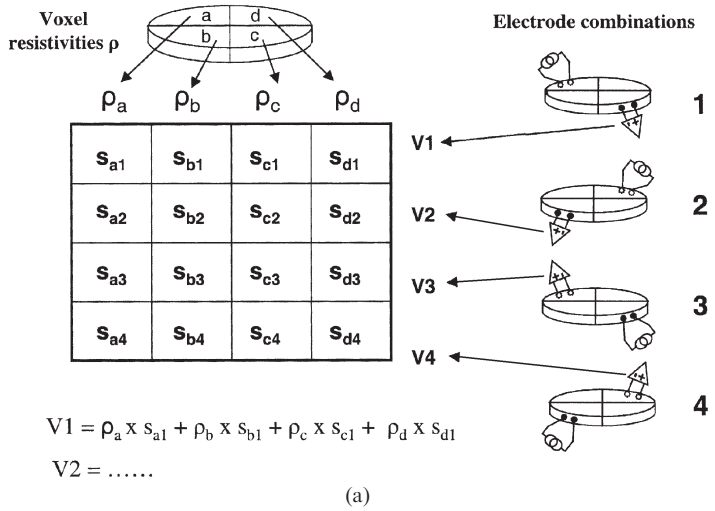

(a)

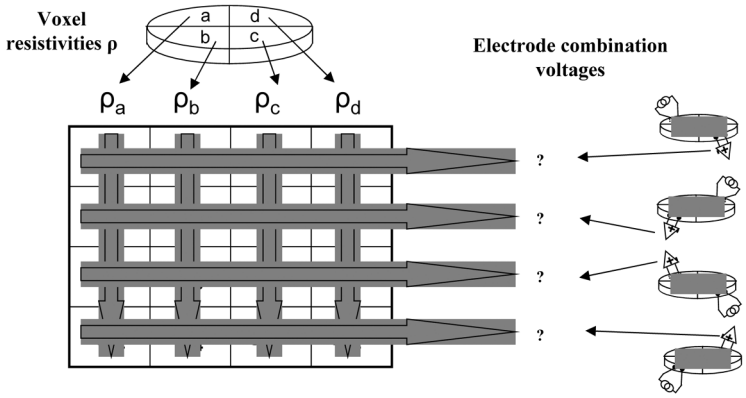

(b)

Figure B.13. Explanation of sensitivity matrix. (a) The sensitivity matrix. This is shown figuratively for a subject with four voxels and four electrode combinations. Each column represents the resistivity of one voxel in the subject. Each row represents the voltage measured for one electrode combination. The current from one current source flows throughout the subject, but the voltage electrodes are most sensitive to a particular volume, shown in grey. The resulting voltage is a sum of the resistivity in each of the voxels weighted by the factor *S* for each voxel, which indicates how much effect that voxel has on the total voltage. (b) The forward case. In a computer program, all the sensitivity factors are calculated in advance. Given all the resistivities for each voxel, the voltages from each electrode combination are easy to calculate. (c) The inverse. For EIT imaging, the reverse is the case—the voltages are known; the goal is to calculate all the voxel resistivities. This can be achieved by 'inverting' the matrix. This is straightforward for the simple case of four unknowns shown here, but is not in a real imaging problem, where the voltages are noisy, and there may be many more unknown voxels than voltages measured.

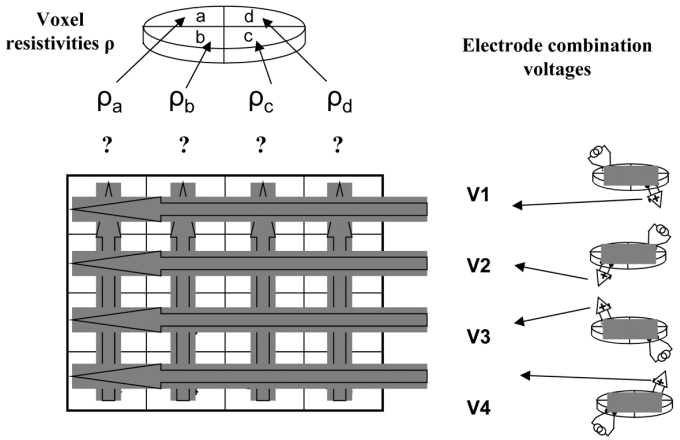

Figure B.13. *(Continued)*

anatomical meshes need to contain many more cells than a few hundred, especially if in 3D, so the matrix may contain tens of thousands of columns—one for each voxel—and a few hundred rows. If the resistivities of each voxel are given, then the expected voltages for each electrode combination may be easily calculated. This is termed the 'forward' solution and is simply a simulation of the situation in reality (figure B.13(b)). Its use is to generate a 'sensitivity matrix'. This is produced by, in a computer simulation, varying resistivity in each voxel, and recording the effect on different voltage recordings. This enables calculation of the sensitivity of a particular voltage recording to resistance change in a voxel—the 's' factor in figure B.13.

To produce an image, it is necessary to reverse the forward solution. On collecting an image data set, the voltages for each electrode combination are known, and, by generating the sensitivity matrix, so is the factor relating each resistance to these. The unknown is the resistivity in each voxel. This is achieved by mathematically inverting the matrix—which yields all the resistivities (figure B.13(c)). In principle, this can give a completely accurate answer, but this is only the case if the data is infinitely accurate, and that there are the same number of unknowns—i.e. voxels requiring resistance estimates, as electrode combinations. In general, none of these is true. In particular, in many of the voxels, very little current passes through, so the sensitivity factor for that cell in the table is near to zero. Just as dividing by zero is impossible, dividing by such very small numbers causes instabilities in the image. This is termed an 'ill-posed' matrix inversion. There is a well established branch of mathematics which deals with these inverse problems, and matrix inversion is made possible by 'regularizing' the matrix. In principle, this is performed by undertaking a noise analysis of the data—noisy channels with little signal-to-noise are suppressed, so that the image production by

inversion relies on electrode combinations with good quality data and so proceeds smoothly. Commonly used methods for this include truncated singular value decomposition (Bagshaw *et al* 2003a) or Tikhonov regularization (Vauhkonen *et al* 1998).

B.3.3. Other developments in algorithms

Initially, reconstruction was always performed with the assumption that the subject was a 2D circle. Although this actually worked quite well in practice, changes in impedance away from the plane of electrodes could be seen in the image, sometimes in an unpredictable way. 3D recording requires far more electrodes—usually four rings of 16 per ring around the chest. For simplicity, many continuing clinical studies still use a 2D approach. The first 3D images were of the chest in 1996 (Metherall *et al* 1996), and an algorithm for imaging in the head has been developed more recently (Bagshaw *et al* 2003a).

The sensitivity matrix approach described above requires an assumption that there is a direct unvarying, or 'linear' relationship, between the resistance of a voxel and its effect on recorded voltage. In practice, this is almost true for small changes in impedance below about 20%. However, it is not true for larger changes. This can be overcome by using more accurate 'non-linear' approaches. This can be achieved by using a logical loop in the algorithm. A guess is made for the initial resistivities in the voxels. The forward solution is calculated to estimate the resulting electrode combination voltages. These are then compared with the original recorded voltage data. The resistances in the model are then adjusted, and the procedure is repeated continuously until the error between the calculated and recorded voltages is minimized to an acceptable level. In theory, this should give more accurate images, but it is time consuming in reconstruction and instabilities may creep in as the process is more sensitive to minor errors, such as anatomical differences between the mesh used and the subject's true anatomy, or the position of electrodes (see Lionheart 2004, Morucci and Marsili 1996, for reviews). Although there is interest in the development of non-linear approaches, the author is not aware of any clinical studies at the time of writing in which they are currently employed.

B.4. CLINICAL APPLICATIONS

B.4.1. Performance of EIT systems

B.4.1.1. Spatial resolution

The great majority of clinical studies have been performed with the Sheffield mark 1 system, so that most published studies of accuracy have mainly been

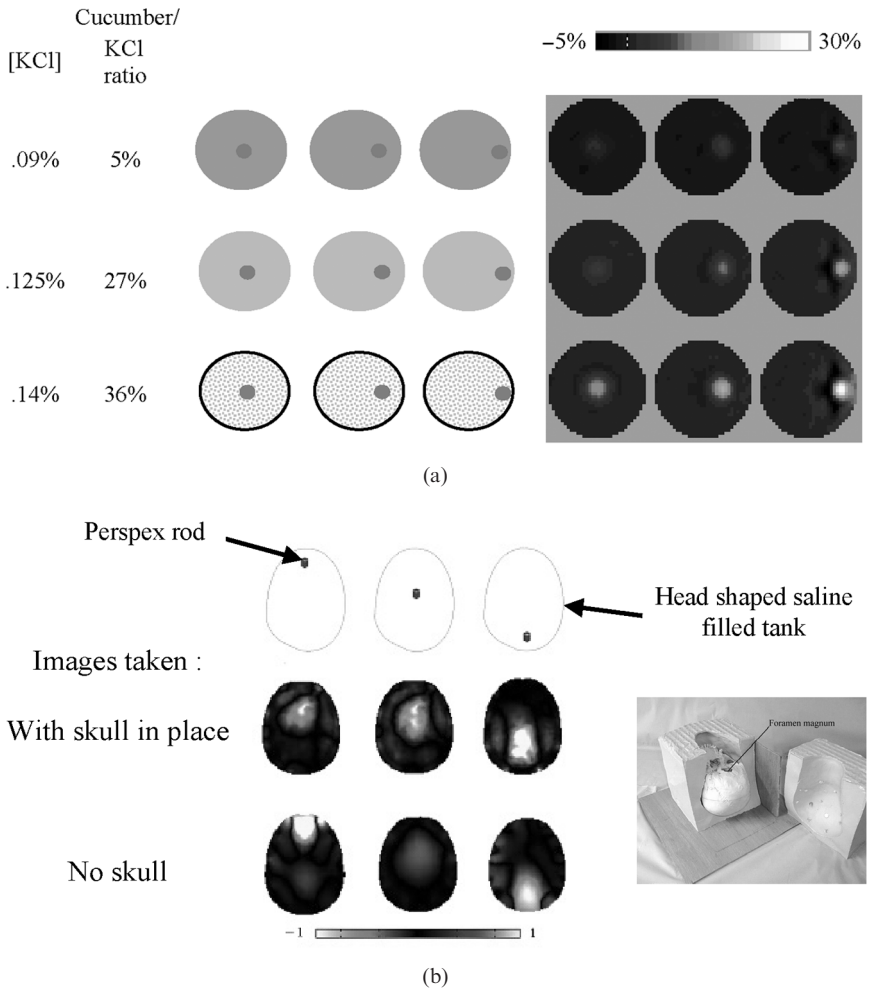

Figure B.14. (a) Calibration studies with the Sheffield mark 1 system in a saline filled tank. The tank was filled with saline, which was varied to give different contrasts with the test object of a cucumber. The cucumber may be seen in the correct location for all contrasts, but with more accuracy and greater change near the edge (Holder *et al* 1996). (b) Images taken with 3D linear algorithm in a latex head-shaped tank, with or without the skull in place. The algorithm employed a geometrically accurate finite element mesh of the skull and tank (Bagshaw *et al* 2003).

with this prototype system. In saline filled tanks, the Sheffield mark 1, with its 16 electrodes and back-projection algorithm, produces somewhat blurred but reproducible images (figure B.14(a)). In general, the spatial accuracy is about 15% of the image diameter, being 12% at the edge and 20% in the centre (see Holder 1993 for a review). More recent studies with more advanced systems,

including those in 3D in the thorax and head, are roughly similar (Metherall *et al* 1996, Bagshaw *et al* 2003b) (figures B.9, B.14(b)). In general, in human images where the underlying physiological change is well described, such as gastric emptying (Mangall *et al* 1987), lung ventilation (Barbas *et al* 2003), lung blood flow (Smit *et al* 2003), or cardiac output (Vonk *et al* 1996), images have a similar resolution with mild blurring, but the anatomical structures can be identified with reasonable confidence. In the more challenging areas such as imaging breast cancer (Soni *et al* 2004), or evoked activity or epileptic seizures in the brain (Tidswell *et al* 2001, Bagshaw *et al* 2003a), some individual images appear to correspond to the known anatomy, but these are not sufficiently consistent across subjects to be used confidently in a clinical environment.

B.4.1.2. Variability

In all dynamic EIT measurements, it is necessary to distinguish the required impedance change from baseline variability. This may be partly due to electronic noise, which may be reduced by averaging as it is random. There may also be systematic changes due to processes such as changes in electrode impedance, temperature or blood volume in body tissues. They may be present as a slowly varying drift, or as irregular variations of shorter duration. In EIT recordings made on exposed cerebral cortex or scalp, a drift of about 0.5% over 10 min was shown to be linear, and was compensated for in images taken over 50 min (Holder 1992a). Murphy *et al* (1987) recorded EIT images from the scalp of infants, and noted that pulse-related impedance changes were about 0.1% in amplitude. Larger irregular changes of about 1% were attributed to movement artefact and respiration. Liu and Griffiths (in Holder 1993) examined baseline variability in EIT images collected from electrodes around the upper abdomen, using their own EIT system which was similar to the Sheffield mark 1 system. Images were collected over 40 min in five subjects. The variations in impedance change were typically 5%, but ranged up to over 20%. Wright *et al* (in Holder 1993) conducted a large study of gastric emptying, in which six different test meals were given to each of 17 subjects; 27% of the tests (28 of 102) were considered 'uninterpretable' and were excluded from the analysis. In all tests in one subject, the region of integral interest was of opposite direction to all the other subjects, so these measurements were discarded. In measurements of gastric emptying following a drink of conducting fluid after acid suppression with cimetidine, baseline variability was usually less than 10% (Avill *et al* 1987).

In general, in dynamic imaging over time, the baseline fluctuates by several per cent over 10 min or so. If the recording takes place over a few minutes or less, or if averaging over time is possible, such as for ventilation or cardiac changes, then images may usually be reliably made.

Variability over time has also been investigated in serial recordings. Gastric emptying times were measured by EIT in eight volunteers after drinking a liquid meal on two successive days (Avill *et al* 1987). Acid production was suppressed by cimetidine. The half emptying times on the two days correlated well ($r = 0.9$). There is a high degree of correlation in cardiac-related lung perfusion changes over both subjects and successive recordings over days (Killingbeck *et al* (in Holder 1993), Smit *et al* 2003).

Variability across subjects is clearly of paramount interest, as it is this which determines how confidently changes seen in an individual patient can be interpreted. In general, there is significant variability, and it is this that has limited the clinical use of EIT. There do not appear to have been quantitative evaluations of this. However, qualitative evaluation, using the Sheffield mark 1 or similar systems, has indicated considerable variability, which may in part be due to variations in electrode position in imaging cardiac output (Patterson *et al* 2001), ventilation (Frerichs 2000) and gastric emptying (Avill *et al* 1987). The most reliable approach has been to extract parameters, such as gastric emptying time, or ventilation ratios, in which the subject acts as their own normalization. Variability in EIT spectroscopy has been investigated in images of neonatal lungs. Changes across frequency were reproducible to within 13% of the highest frequency, 1.2 MHz, was eliminated, but Cole parameters, such as centre frequency, were excessively variable across subjects (Marven *et al* 1996).

B.4.2. Potential clinical applications

B.4.2.1. Gastrointestinal function

Measurement of gastric emptying can be useful clinically in disorders of gastrointestinal motility. Imaging gastric emptying was one of the earliest proposed applications of EIT and has been validated as a reliable method (Mangall *et al* 1987, Ravelli *et al* 2001). It is now used in clinical research, but still at a few specialist centres with EIT expertise. Although it appears to have the potential for widespread use, this has not yet happened, largely because good, although invasive, alternative methods are available, such as radioisotope scintigraphy. Good pilot studies have also demonstrated its utility in imaging in pyloric stenosis (Nour *et al* 1993) and acid reflux (Ravelli and Milla 1994), but this early interest does not appear to developed into clinical use.

B.4.2.2. Thoracic imaging of lung and cardiac function

The clinical application which has received the greatest interest has been imaging of lung ventilation and cardiac output (Frerichs 2000). Large impedance changes occur during ventilation, as air enters and leaves the

lungs. Although the images have a relatively low resolution, several pilot studies have confirmed that reasonably accurate data concerning ventilation can be continuously obtained at the bedside (Harris *et al* 1988, Kunst *et al* 1998). EIT therefore has the potential to image ventilation. Although the feasibility of imaging this with the Sheffield mark 1 system was established in the 1980s, the method has not yet been taken up into clinical use. This is presumably because good imaging methods already exist for assessing lung function and pathology, and the portability of EIT was not considered sufficient to outweigh relatively poor spatial resolution. However, recently, there has been fresh interest in this application, led by Amato and colleagues (Kunst *et al* 1998, Barbas *et al* 2003, Hinz *et al* 2003, Victorino *et al* 2004). In operating theatres or Intensive Care Units, there is a growing body of thought that, in ventilated patients, the outcome is improved if ventilation is adjusted so that no regions of lung stay collapsed; EIT is sufficiently small and rapid to enable continuous monitoring at the bedside to achieve this.

Pilot studies have also shown that EIT has reasonable accuracy in imaging in emphysema (Eyuboglu *et al* 1995), pulmonary oedoema (Noble *et al* 1999), lung perfusion with gating of recording to the ECG (Smit *et al* 2003), and perfusion during pulmonary hypertension (Smit *et al* 2002). However, although of physiological interest, these applications have not yet been taken up as being sufficiently accurate for clinical use.

All the above studies have employed the Sheffield mark 1 or similar 2D systems with a single ring of electrodes; it appears that this gives sufficient resolution to enable optimization of ventilator settings when compared to concurrent CT scanning (Victorino *et al* 2004). Studies have also been performed in the thorax with more advanced methods. A method for 3D imaging of lung ventilation created great interest on publication in 1996 (Metherall *et al* 1996), but this requires the use of four rings of 16 electrodes each and has not been taken up for further clinical studies, presumably because of practical difficulties in applying this number of electrodes in critically ill subjects. The above studies have used EIT at a single frequency and relied on its anatomical imaging capability for the proposed clinical use. An alternative philosophy, developed in the Sheffield group, has been to go to lower spatial resolution and extract EITS parameters of the lung function in conditions such as respiratory distress or pulmonary oedoema, on the principle that such conditions diffusely affect the lung and the method will be more reliable. The characteristics of adult (Brown *et al* 1995) and neonatal (Brown *et al* 2002) lungs have been obtained in normal subjects, but this has yet to be taken up in further studies in pathological conditions.

B.4.2.3. Breast tumours

Early diagnosis by screening of the common condition of breast cancer is another area where the portability of EIT could lead to benefits. The

electrical properties of breast tumours may differ significantly from the surrounding tissue and could enable EIT to be effective in screening. At present, women are screened for breast cancer using x-ray mammography, though some cancers of the breast cannot be seen using this technique. During this procedure, their breast is compressed flat in order to visualize all the tissue and minimize the required radiation dose—this can be uncomfortable and sometimes painful for the patient. There is also a high false-positive rate of 40% and the false-negative rate is 26%. Preliminary clinical images have been collected by groups in Dartmouth, USA (Soni *et al* 2004), and Moscow (Cherepenin *et al* 2002), but whether it will prove sufficiently sensitive and spatially accurate is not yet clear.

B.4.2.4. Brain function

There are already excellent methods for imaging brain anatomy and function—x-ray CT, MRI and functional MRI. EIT has the potential, however, to offer a low-cost portable system for imaging brain abnormalities like epileptic activity or stroke, where it is not practicable to undertake serial or rapid imaging in a large scanner. For example, it could enable take-up of a new treatment for stroke. New thrombolytic ('clot-busting') drugs have been shown to improve outcome in acute stroke, but must be administered within three hours of the onset. Neuroimaging must be performed first, in order to determine the cause of the stroke; about 15% of strokes are due to a haemorrhage, and thrombolysis must not be given in these patients, as it may make the haemorrhage extend. In practice, it is not possible to obtain and report a CT scan in the recommended 30 min. EITS could be available in casualty departments and used to provide images which would enable distinction of haemorrhagic from ischaemic stroke, and so enable the rapid use of thrombolytic drugs. It also has the potential for imaging the small impedance changes associated with opening of ion channels during activity in the brain, which is not presently possible by any other method and would be substantial advance. Unfortunately, EIT of the brain has to overcome the difficulty of injecting current through the resistive skull.

Systems optimized for brain imaging have been developed at University College London. Imaging through the skull with reasonably good resolution has been shown to be possible, mainly by using widely spaced electrodes for current injection (Bagshaw *et al* 2003a). A series of pilot studies in anaesthetized animals with electrodes placed directly on the brain, and the Sheffield mark 1 system, confirmed that suitable changes could be imaged in stroke (Holder 1992b), epilepsy (Rao *et al* 1997) and evoked activity (Holder *et al* 1996b). In humans, with recording in 3D using scalp electrodes, reproducible impedance changes have been recorded during physiologically evoked activity (Tidswell *et al* 1999) and epilepsy (Fabrizi *et al* 2004), but

the reconstructed images were noisy and did not reveal consistent changes. At the time of writing, trials are in progress to assess the utility of EIT in acute stroke and epilepsy with improved multifrequency hardware and reconstruction algorithms.

B.5. CURRENT DEVELOPMENTS

This review has covered applications with conventional EIT. There are two new methods, with considerable potential, which are still in technical development, and have not yet been used for clinical studies. Magnetic induction tomography (MIT) is similar in principle to EIT, but injects and records magnetic fields from coils. It has the advantages that the position of the coils is accurately known and there is no skin-electrode impedance, but the systems are bulkier and heavier than EIT. In general, higher frequencies have to be injected in order to gain a sufficient signal-to-noise ratio. Until now, spatial resolution has been the same or worse than EIT. The method could offer advantages in imaging brain pathology, as magnetic fields pass through the skull, and may in the thorax or abdomen if the method can be developed to demonstrate improved sensitivity over EIT. MR-EIT (magnetic resonance-EIT) requires the use of an MRI scanner. Current is injected into the subject and generates a small magnetic field that alters the MRI signal. The pattern of resistivity in three dimensions may be extracted from the resulting changes in the MRI images. This therefore loses the advantage of portability in EIT, but has the great advantage of high spatial resolution of MRI. It could be used to generate accurate resistivity maps for use in models for reconstruction algorithms in EIT, especially for brain function, where prior knowledge of anisotropy is important.

Biomedical EIT is, at the time of writing, in a phase of consolidation, where optimized EIT systems are still being assessed in new clinical situations. Almost all clinical studies have been undertaken with variants of the 2D Sheffield mark 1 system. Several groups are near completion of more powerful systems with improved instrumentation and reconstruction algorithms, with realistic anatomical models and non-linear methods. The most promising applications appear to be in breast cancer screening, optimization of ventilator settings in ventilated patients, brain pathology in acute stroke and epilepsy, and gastric emptying. Although there is a commercial application in breast cancer screening with an impedance scanning device, EIT has yet to fulfil its promise in delivering a robust and widely accepted clinical application. Well funded clinical trials are in progress in the above applications, and there seems to be a reasonable chance that one or more, especially if using improved technology, may prove to be the breakthrough.

REFERENCES

Avill R, Mangnall Y F, Bird N C, Brown B H, Barber D C, Seagar A D, Johnson A G and Read N W 1987 Applied potential tomography. A new noninvasive technique for measuring gastric emptying *Gastroenterology* **92** 1019–1026

Bagshaw A P, Liston A D, Bayford R H, Tizzard A, Gibson A P, Tidswell A T, Sparkes M K, Dehghani H, Binnie C D and Holder D S 2003 Electrical impedance tomography of human brain function using reconstruction algorithms based on the finite element method *Neuroimage* **20** 752–764

Baisch F J 1993 Body fluid distribution in man in space and effect of lower body negative pressure treatment *Clin. Investig.* **71** 690–699

Barbas C S, de Matos G F, Okamoto V, Borges J B, Amato M B and de Carvalho C R 2003 Lung recruitment maneuvers in acute respiratory distress syndrome *Respir. Care Clin. N. Am.* **9** 401–418, vii

Benabid A L, Balme L, Persat J C, Belleville M, Chirossel J P, Buyle-Bodin M, de Rougemont J and Poupot C 1978 Electrical impedance brain scanner: principles and preliminary results of simulation *TIT. J. Life Sci.* **8** 59–68

Boone K, Barber D and Brown B 1997 Imaging with electricity: report of the European Concerted Action on Impedance Tomography *J. Med. Eng Technol.* **21** 201–232

Boone K G and Holder D S 1996 Current approaches to analogue instrumentation design in electrical impedance tomography *Physiol Meas.* **17** 229–247

Brown B and Seagar A 1987 The Sheffield data collection system *Clinical Physics and Physiological Measurements* **8** 91–97

Brown B H 2003 Electrical impedance tomography (EIT): a review *J. Med. Eng Technol.* **27** 97–108

Brown B H, Leathard A D, Lu L, Wang W and Hampshire A 1995 Measured and expected Cole parameters from electrical impedance tomographic spectroscopy images of the human thorax *Physiol Meas.* **16** A57–A67

Brown B H, Primhak R A, Smallwood R H, Milnes P, Narracott A J and Jackson M J 2002 Neonatal lungs: maturational changes in lung resistivity spectra *Med. Biol. Eng Comput.* **40** 506–511

Cherepenin V A, Karpov A Y, Korjenevsky A V, Kornienko V N, Kultiasov Y S, Ochapkin M B, Trochanova O V and Meister J D 2002 Three-dimensional EIT imaging of breast tissues: system design and clinical testing *IEEE Trans. Med. Imaging* **21** 662–667

Cook R D, Saulnier G J, Gisser D G, Goble J C, Newell J C and Isaacson D 1994 ACT3: a high-speed, high-precision electrical impedance tomograph *IEEE Trans. Biomed. Eng* **41** 713–722

Eyuböğlu B M, Oner A F, Baysal U, Biber C, Keyf A I, Yilmaz U and Erdogan Y 1995 Application of electrical impedance tomography in diagnosis of emphysema—a clinical study *Physiol Meas.* **16** A191–A211

Fabrizi L, Sparkes M, Holder D S, Yerworth R, Binnie C D and Bayford R 2004 Electrical Impedance Tomography (EIT) During Epileptic Seizures: Preliminary Clinical Studies. XII International Conference on Bioimpedance and Electrical Impedance Tomography, Gdansk, Poland

Fitzgerald A J, Holder D S, Eadie L, Hare C and Bayford R H 2002 A comparison of techniques to optimize measurement of voltage changes in electrical impedance tomography by minimizing phase shift errors *IEEE Trans. Med. Imaging* **21** 668–675

Frerichs I 2000 Electrical impedance tomography (EIT) in applications related to lung and ventilation: a review of experimental and clinical activities *Physiol Meas*. **21** R1–R21

Halter R, Hartov A and Paulsen K D 2004 Design and implementation of a high frequency electrical impedance tomography system *Physiol Meas*. **25** 379–390

Hampshire A R, Smallwood R H, Brown B H and Primhak R A 1995 Multifrequency and parametric EIT images of neonatal lungs *Physiol Meas*. **16** A175–A189

Harris N D, Suggett A J, Barber D C and Brown B H 1988 Applied potential tomography: a new technique for monitoring pulmonary function *Clin. Phys. Physiol Meas*. **9** Suppl A 79–85

Henderson R P and Webster J G 1978 An impedance camera for spatially specific measurements of the thorax *IEEE Trans. Biomed. Eng* **25** 250–254

Hinz J, Hahn G, Neumann P, Sydow M, Mohrenweiser P, Hellige G and Burchardi H 2003 End-expiratory lung impedance change enables bedside monitoring of end-expiratory lung volume change *Intensive Care Med*. **29** 37–43

Holder D 1993 *Clinical and physiological applications of electrical impedance tomography*. UCL Press, London

Holder D S 1992a Detection of cerebral ischaemia in the anaesthetised rat by impedance measurement with scalp electrodes: implications for non-invasive imaging of stroke by electrical impedance tomography *Clin. Phys. Physiol Meas*. **13** 63–75

Holder D S 1992b Electrical impedance tomography with cortical or scalp electrodes during global cerebral ischaemia in the anaesthetised rat *Clin. Phys. Physiol Meas*. **13** 87–98

Holder D S, Hanquan Y and Rao A 1996a Some practical biological phantoms for calibrating multifrequency electrical impedance tomography *Physiol Meas*. **17** Suppl 4A A167–A177

Holder D S, Rao A and Hanquan Y 1996b Imaging of physiologically evoked responses by electrical impedance tomography with cortical electrodes in the anaesthetised rabbit *Physiological Measurement* **17** A179–A186

Kunst P W, Vonk N A, Hoekstra O S, Postmus P E and de Vries P M 1998 Ventilation and perfusion imaging by electrical impedance tomography: a comparison with radionuclide scanning *Physiol Meas*. **19** 481–490

Lionheart W R 2004 EIT reconstruction algorithms: pitfalls, challenges and recent developments *Physiol Meas*. **25** 125–142

Mangall Y, Baxter A, Avill R, Bird N, Brown B, Barber D, Seager A, Johnson A and Read N 1987 Applied Potential Tomography: a new non-invasive technique for assessing gastric function *Clinical Physics and Physiological Measurement* **8** 119–129

Marven S S, Hampshire A R, Smallwood R H, Brown B H and Primhak R A 1996 Reproducibility of electrical impedance tomographic spectroscopy (EITS) parametric images of neonatal lungs *Physiol Meas*. **17** Suppl 4A A205–A212

McAdams E T, McLaughlin J A and McC A J 1994 Multi-electrode systems for electrical impedance tomography *Physiol Meas*. **15** Suppl 2A A101–A106

Metherall P, Barber D C, Smallwood R H and Brown B H 1996 Three-dimensional electrical impedance tomography *Nature* **380** 509–512

Morucci J P and Marsili P M 1996 Bioelectrical impedance techniques in medicine. Part III: Impedance imaging. Second section: reconstruction algorithms *Crit Rev. Biomed. Eng* **24** 599–654

Murphy D, Burton P, Coombs R, Tarassenko L and Rolfe P 1987 Impedance imaging in the newborn *Clin. Phys. Physiol Meas.* **8** Suppl A 131–140

Noble T J, Morice A H, Channer K S, Milnes P, Harris N D and Brown B H 1999 Monitoring patients with left ventricular failure by electrical impedance tomography *Eur. J. Heart Fail.* **1** 379–384

Nour S, Mangnall Y, Dickson J A, Pearse R and Johnson A G 1993 Measurement of gastric emptying in infants with pyloric stenosis using applied potential tomography *Arch. Dis. Child* **68** 484–486

Patterson R P, Zhang J, Mason L I and Jerosch-Herold M 2001 Variability in the cardiac EIT image as a function of electrode position, lung volume and body position *Physiol Meas.* **22** 159–166

Rao A, Gibson A and Holder D S 1997 EIT images of electrically induced epileptic activity in anaesthetised rabbits. *Med & Biol. Eng & Comp.* **35** 3274

Ravelli A M and Milla P J 1994 Detection of gastroesophageal reflux by electrical impedance tomography *J. Pediatr. Gastroenterol. Nutr.* **18** 205–213

Ravelli A M, Tobanelli P, Volpi S and Ugazio A G 2001 Vomiting and gastric motility in infants with cow's milk allergy *J. Pediatr. Gastroenterol. Nutr.* **32** 59–64

Smit H J, Vonk N A, Roeleveld R J, Bronzwaer J G, Postmus P E, de Vries P M and Boonstra A 2002 Epoprostenol-induced pulmonary vasodilatation in patients with pulmonary hypertension measured by electrical impedance tomography *Physiol Meas.* **23** 237–243

Smit H J, Handoko M L, Vonk N A, Faes T J, Postmus P E, de Vries P M and Boonstra A 2003 Electrical impedance tomography to measure pulmonary perfusion: is the reproducibility high enough for clinical practice? *Physiol Meas.* **24** 491–499

Soni N K, Hartov A, Kogel C, Poplack S P and Paulsen K D 2004 Multi-frequency electrical impedance tomography of the breast: new clinical results *Physiol Meas.* **25** 301–314

Tidswell A, Bagshaw A, Holder D, Yerworth R, Eadie L, Murray S, Morgan L and Bayford R 2003 A comparison of headnet electrode arrays for electrical impedance tomography of the human head *Physiological Measurement* **24** 1–18

Tidswell T, Gibson A, Bayford R H and Holder D S 2001 Three-dimensional electrical impedance tomography of human brain activity *Neuroimage* **13** 283–294

Vauhkonen M, Vadasz D, Karjalainen P A, Somersalo E and Kaipio J P 1998 Tikhonov regularization and prior information in electrical impedance tomography *IEEE Trans. Med. Imaging* **17** 285–293

Victorino J A, Borges J B, Okamoto V N, Matos G F, Tucci M R, Caramez M P, Tanaka H, Sipmann F S, Santos D C, Barbas C S, Carvalho C R and Amato M B 2004 Imbalances in regional lung ventilation: a validation study on electrical impedance tomography *Am. J. Respir. Crit Care Med.* **169** 791–800

Vonk N A, Faes T J, Marcus J T, Janse A, Heethaar R M, Postmus P E and de Vries P M 1996 Improvement of cardiac imaging in electrical impedance tomography by means of a new electrode configuration *Physiol Meas.* **17** 179–188

Yerworth R J, Bayford R H, Cusick G, Conway M and Holder D S 2002 Design and performance of the UCLH mark 1b 64 channel electrical impedance tomography (EIT) system, optimized for imaging brain function *Physiol Meas.* **23** 149–158

Yerworth R J, Bayford R H, Brown B, Milnes P, Conway M and Holder D S 2003 Electrical impedance tomography spectroscopy (EITS) for human head imaging *Physiol Meas* **24** 477–489

Zhu Q, Lionheart W R, Lidgey F J, McLeod C N, Paulson K S and Pidcock M K 1993 An adaptive current tomography using voltage sources *IEEE Trans. Biomed. Eng* **40** 163–168

Zhu Q S, McLeod C N, Denyer C W, Lidgey F J and Lionheart W R 1994 Development of a real-time adaptive current tomograph *Physiol Meas.* **15** Suppl 2A A37–A43